Arch. Mech., 43, 5, pp. 669–689, Warszawa 1991

Effects of strong temperature gradients on turbulent wakes

A. A. SZEWCZYK and T.F. TUREAUD (NOTRE DAME)

THE EFFECTS of stable and unstable thermal stratification on the development of a turbulent wake were considered. A turbulence wake behind an insulated splitter plate was subjected to thermal stratification caused by strong grid heating at Brunt–Väisälä frequencies in the range 2.0–6.0 rad/s^{-1}. At large Brunt–Väisälä frequencies the dynamically active buoyancy forces altered the development of the turbulent structure and led to significantly modified vertical and horizontal heat flux distributions and fluctuating energy densities.

1. Introduction

TURBULENCE in stratified media is a phenomenon common to variety of meteorological, geophysical and engineering problems. Oceanic and atmospheric microstructural transport common to problems in environmental engineering in nuclear and fossil fuel plant thermal discharges for example, or the interaction of propelled or self-propelled bodies in the presence of strong stratification are specific problems which require an understanding of what role dynamically active buoyancy forces play in the presence of turbulence. The exact role that dynamically active buoyancy forces play in the development of a turbulent motion with its features can be characterized and it is the purpose of this paper to review our present understanding and put forth some new results.

In the problem referred to above one generally deals with free-turbulent shear flows such as the jet, the mixing region and wake flows. Our present understanding of jets is largely due to the early investigation of CORRSIN [27], CORRSIN and UBEROI [28], BRADBURY [15], WYGNANSKI and FIELDER [85], GOLDSCHMIDT and YOUNG [36], JENKINS [39], KOTSOVINAS [42], GUTMARK and WYGNANSKI [38] and more recently by HUSSAIN and ZAMAN [89] and COHEN, GUTMARK and WYGNANSKI [26].

The mixing region has been studied by LIEPMANN and LAUFER [47], BROWAND [16], WYGNANSKI and FIELDER [86], and SPENCER [67]. Others who have reported on the fundamental aspects of the stability and structure of the mixing layer have been BROWAND and WEIDMAN [17], DIMOTAKIS and BROWN [30], ROSHKO [64], [65], BERNAL [14], and BROWAND and HO [18].

The third of the major classes of turbulent shear flows, wakes, has been the focus of numerous experimental investigations. For detailed review of the subject, the reader is referred to MORKOVIN [54] and BERGER and WILLE [13]. The majority of experimental efforts in the past have dealt primarily with near wake flows. Investigations of the near wake of a circular cylinder were pioneered by KOVASZNAY [43] and ROSHKO [63]. The present paper will not deal with near wakes but with the intermediate and far wakes of bluff body generators. In particular special attention will be paid to the effects of strong temperature gradients on the growth, turbulent structure and self-preserving properties of a wake. While small temperature effects or passive contaminants which arise from heated bodies will be discussed, the purpose of this paper is to stress how significant temperature differences alter the flow characteristics far downstream. It will be shown that significant

changes occur in the higher order correlations as well as turbulent structure of the flow as evidenced by the changes in u't' and v't' distributions, the streamwise and longitudinal heat fluxes distributions respectively, and the turbulent kinetic energy. To set a basis for our results a brief review of some important far wake investigations will be presented.

2. Brief review of turbulent wakes

2.1. Isothermal wakes

The flow structure and characteristics of asymptotic plane turbulent far wakes, e.g. see Fig. 1a, have been described by very simple classical theories. Excellent experimental data exist for asymptotic two-dimensional wakes starting with those reported by TOWNSEND [76, 75, 77, 78] in which he measured the mean and fluctuating magnitude of all three velocity components, the Reynolds stresses, as well as the transport of heat and kinetic energy at a number of downstream stations. These early works were followed by that of GRANT [37] who investigated the flow structure and put forth the idea that two types of large scale motions existed in the wake. One of these is a pair of vortices, side by side and rotating in opposite directions with axes aligned approximately normal to the plane of the wake. The other being a series of jets in which turbulent fluid is projected outward from the core of the wake.

Data of ALEXOPOULOS and KEFFER [1] and THOMAS [74] supported Townsend's earlier findings for the most part. Although some discrepancies were found in Townsend's original data the idea of self-preservation in the sense of TOWNSEND [79] was confirmed. Further, the investigations of UBEROI and FREYMUTH [83], SYMES and FINK [70] and YAMADA, KAWATA, OSAKA and KAGEYAMA [88] reaffirmed that wake flows were self-preserving and that the velocity and length scales, U_0 and L_0, vary as $(x - x_0)^{-1/2}$ and $(x - x_0)^{1/2}$, respectively. On the other hand, KEFFER [40,41] considered the changes in a two-dimensional turbulent wake under the constraint of strain and found that the classical self-preserving technique could be applied only to rather simple flow situations and flows with external strain field do not belong to this class. Similarly, NARASHIMA and PRABHU [56] observed behaviour of wake to be appreciably different when the pressure gradient is not very small and the self-preservation will exhibit equilibrium only if the relaxation length is small compared with the characteristic streamwise length of the flow.

A further look at self-preservation was reported by SREENIVASAN [68] who showed that plane turbulent wakes behind wake generators of differing shape approach a unique self-preservation state, suggesting that all the wakes — no mater how created — quickly attain the same shape of mean velocity profile. He observed that each flow preserved the shape of the mean velocity profile when normalized by its own characteristic scale even though they had their own and different natural process of development. It was then that SREENIVASAN and NARASHIMA [69] put forward for consideration a thought that a unique self-preserving state exists for all plane wakes, and velocity and length scales which are universal constants result.

Results of recent work by WYGNANSKI, CHAMPAGNE and MARASLI [87] indicate that the normalized characteristic velocity and length scales for two-dimensional, turbulent, small deficit wakes for various wake generators depend on initial conditions while the shape of the normalized mean velocity profile is independent of these conditions and the nature of the generator. So that, in the sense of TOWNSEND [79] the mean velocity

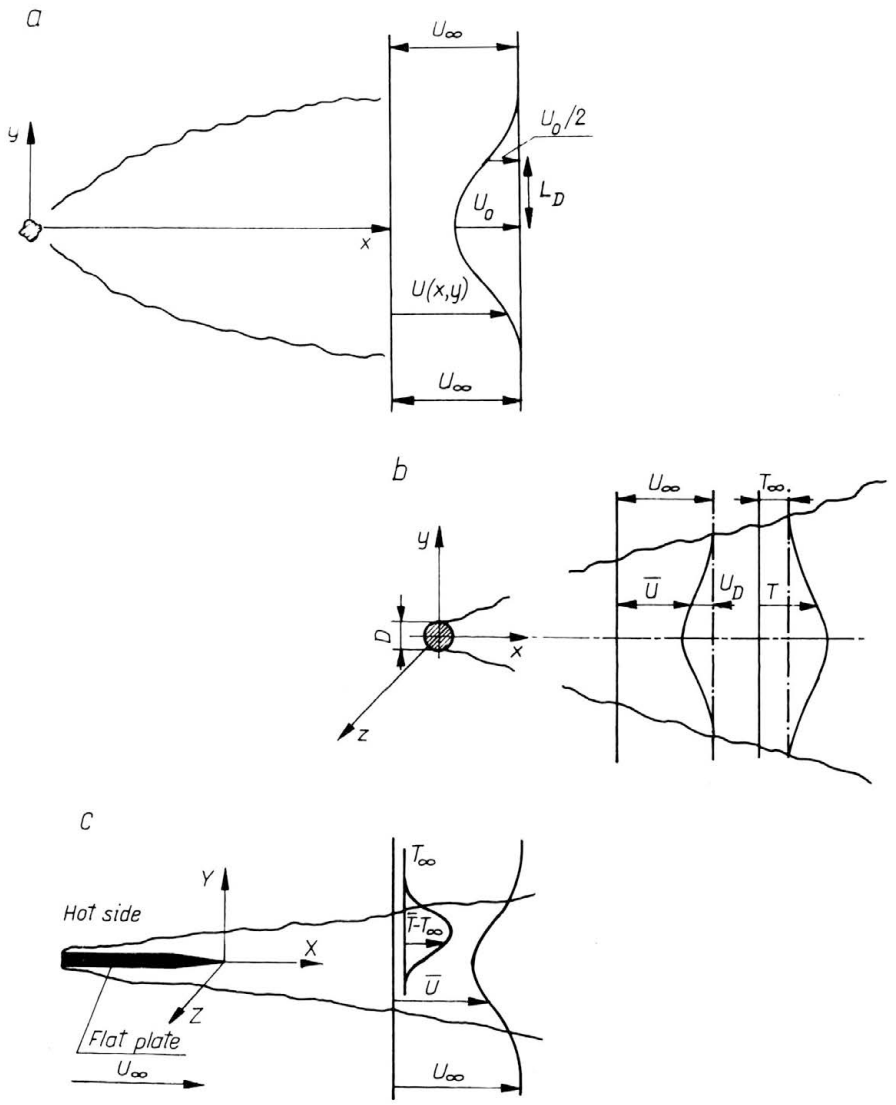

FIG. 1. Turbulent wake generator configurations; a) isothermal flow, b) symmetrically heated wake flow, c) nonsymmetrically heated flow.

profiles, for each wake, when normalized by their own velocity and length scaled are self-preserving while the characteristic velocity and length scales when suitably scaled by the momentum thickness do not exhibit universal behaviour.

Aside from the issue of self-preservation, much effort has been gone into determining the topology of large organized and coherent structures in the far wake. Their existence from hot-wire measurements was first noted by GRANT [37], followed by KEFFER [40], TOWNSEND [80] and MUMFORD [55], and through the use of flow visualization by TANEDA

[71], KEFFER [40], PAPAILIOU and LYKOUDIS [59] and CLIMBALA [23, 24]. For a detailed review and present state-of-the-art of organized structures behind bluff bodies the reader is referred to the recent papers of ANTONIA, BROWNE and BISSET [7] and CIMBALA, NAGIB and ROSHKO [25].

2.2. Thermally heated wakes

As with isothermal wakes, there have been numerous investigations of wakes in the presence of a temperature field. Varied configurations as shown in Figs. 1b and 1c and indicated in Table 1. Most investigations cited have dealt with stratification conditions in which the temperature was a passive scalar contaminant and as a result buoyancy effects could be neglected. For example, in the investigation reported by WARHAFT and LUMLEY [84], the temperature range reported was 25 – 35°C. This was the local temperature difference which gave rise to decaying passive temperature fluctuations so that buoyancy effects could be neglected. In a number of the other investigations cited, the temperature scalar was used merely as a tracer for the study of the flow structure.

In two of the investigations listed, LIENHARD and VAN ATTA [46] and TUREAUD [81] as reported by TUREAUD, SZEWCZYK, NEE and YANG [82] strong temperature gradients have been imposed on the flow in either stable or unstable configurations. These lead to large Brunt–Väisälä frequencies, $Nb = (g/T\partial T/\partial z)^{1/2}$, in the range of 2.0 – 6.0 rad/s, which could be maintained and studied. The approaches to obtain large temperature gradients or equivalently large Brunt–Väisälä frequencies were quite different. However, some similar and confirming results were obtained for two different problems investigated.

In the LIENHARD and VAN ATTA [46] investigation a novel wind tunnel produces strong thermal stratification in a steady, uniform mean flow by using a variable electric heat exchanger. Linear temperature gradients of up to 200°C/m (Brunt—Väisälä frequencies of 2.5 rad/s) could be sustained. Grid-generated turbulence in the presence of strong thermal stratification was studied in this tunnel. It was found that the turbulence is characterized as two-scale process dominated by buoyancy forces at large scales of motion and dissipative effects at small scales. Buoyancy effects on the vertical heat flux, the vertical velocity, the scalar variance and the dissipation rates were scaled with a buoyancy time scale to produce universal curves. Buoyancy forces strongly retarded the vertical dispersion of fluid particles causing marked reductions in the vertical kinetic energy and the vertical transport of heat. The loss of vertical kinetic energy to buoyant potential energy led to anisotropy in the velocity field. The suppression of vertical turbulent motions also strongly suppressed the vertical heat flux. The declining transport in the flow was found to be related to levels of the rms kinetic and potential energy characterized by the buoyancy length scale associated with kinetic energy and the overturning length scale associated with potential energy. Some of these same features were found in the investigations reported by TUREAUD [81], and TUREAUD, SZEWCZYK, NEE and YANG [82] and further reported on in the present paper.

3. Experimental details

3.1. Present investigation

The present experimental investigation considers the development of the velocity field of a turbulent wake behind a splitter plate in the presence of a thermal field. The tempera-

Table 1.

Author	Type of flow	U, mean velocity (m/s)	Temperature Characteristic L (cm)	difference ΔT(°C)
NICHOLL [57]	Boundary layer	1.5–2.4	3	20–100
ARYA [10]	Boundary layer	3–9	50–75	43
SCHON *et al.* [66]	Boundary layer	3–20	$\delta \sim 5 - 10$	40–80
ANTONIO *et al.* [8]	Boundary layer	9.45	$\delta \sim 8$	12
REY *et al.* [62]	Boundary layer	1–20	$\delta \sim 20$	80
WARHAFT and LUMLEY [84]	Grid turbulence	6.5	2.5	25–35
TAVOULARIS and CORRSIN [72]	Shear flow	12.5	$\lambda \sim 0.5$	1–2
LIENHARD and VAN ATTA [46]	Grid turbulence	2–5	$\lambda \sim 0.015 - 0.5$	20–50
KEFFER [40]	Mixing layer	15.4	1–10	33
FIEDLER [1974]	Mixing layer	8	0.8	26
ANTONIA and VAN ATTA [5]	Jet	7.94	2.45	3.3
DAVIES *et al.* [29]	Jet	13.5	5	14.6
ALEXOPOULOS and KEFFER [1]	Wake, cylinder	5	1.27–2.54	0.22°C/cm
LA RUE and LIBBY [44]	Wake, cylinder	7.6	0.66	Low
FABRIS [31,32]	Wake, cylinder	6.5	0.63	0.34
OOSTHUIZEN [58]	Wake, cylinder	0.41–0.59	2(dia)	37–64
BARSOUM *et al.* [12]	Wake, cylinder	10	0.6	4.5
BOLONOV and LOBACHER [11]	Wake, cylinder	0.01–0.1	6	10–45
TAVOULARIS and SREENIVASAN [73]	Wake, cylinder	6.6	1.1	Low
ANTONIA *et al.* [6,7,8,9]	Wake, cylinder	6.5	1.23	0.82
BROWNE *et al.* [19]	Wake, cylinder	6.7	0.267	Low
FARRE and GIRALT [33]	Wake, cylinder	2–20	1.2	1°K
ALI and KOVASZNAY [2]	Wake, plate	3.8	$\delta_{tr} = 5$	10–20
MOREL *et al.* [51,52,53]	Wake, plate	10.6	$\delta_T = 4.4$	25
ANDREOPOULOS and BRADSHAW [3]	Wake, plate	33	$\delta_m \sim 0.5$	1.5–2
TUREAUD, SZEWCZYK *et al.* [82]	Wake, plate	7	$\delta_m \sim 0.25 - 0.5$	0–50

ture field is generated by uniformly heating the air flow either above or below a splitter plate. The upper and lower flow fields interact at the trailing edge of the plate as shown in Fig. 2a. In this way a step function in temperature is imposed onto the wake flow at trailing edge and then allowed to develop downstream along with the velocity field.

3.2. Experimental arrangement

A splitter plate, shown in Fig. 2b, used to generate a turbulent wake was constructed from glass which acted as an insulator between the upper and lower flows. Attached to the end of the glass plate was a tapered 0.15 m length of aluminium which provided a

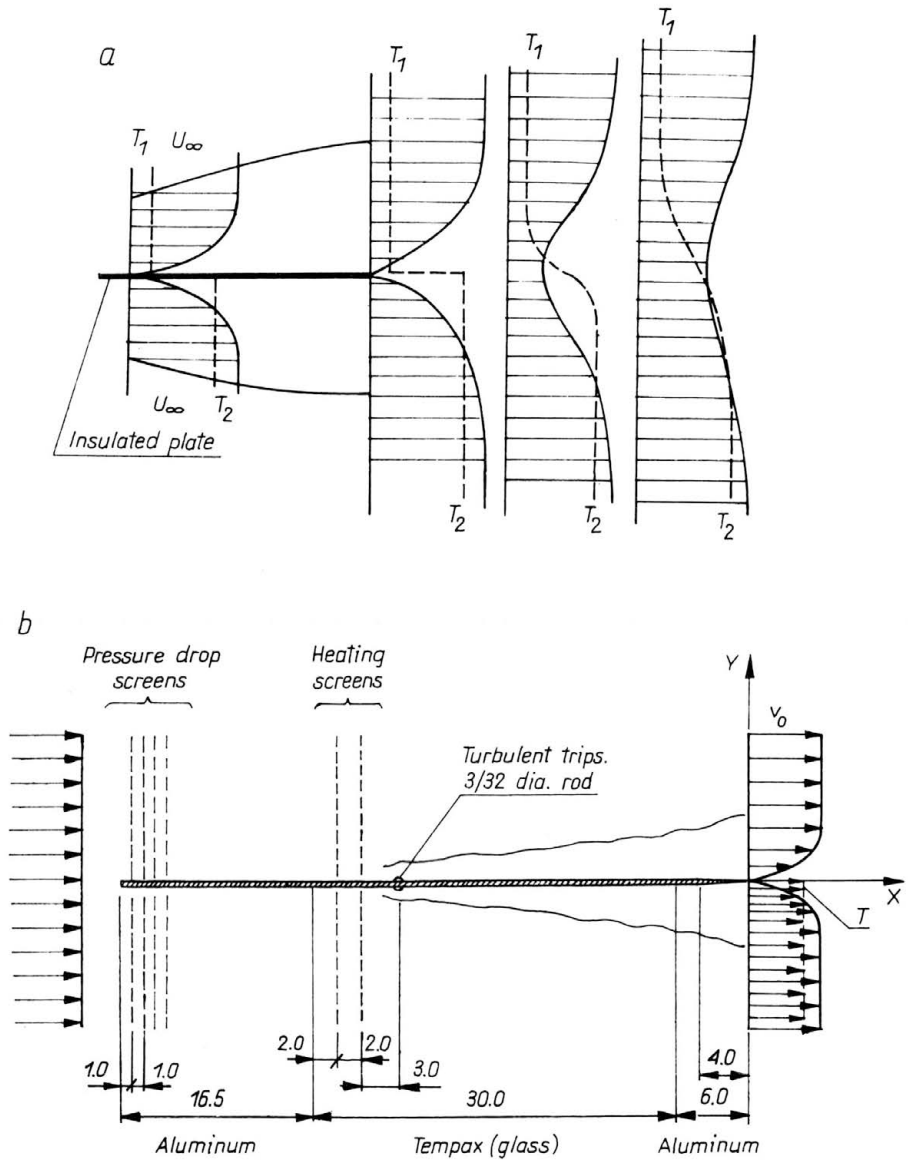

FIG. 2. Splitter plate wake generator.

sharp trailing edge. The plate had dimensions of $1 \times 0.4 \times 0.006$ m, and was mounted horizontally in a 0.4×0.4 m working section of a low speed wind tunnel. The tunnel was an open return pusher type driven by a 10 hp electric motor turning a two stage axial fan.

The flow was heated either above or below the plate by a series of four electrically heated 20 mesh nichrome wire screens. The maximum available electric power of 30 kw was supplied by constant potential welding power supply. Temperature differences ranging

from 0 – 40°C were investigated at freestream velocity of 7 m/s. Other details about the experimental apparatus, arrangement and data acquisition can be found in TUREAUD *et al.*, [82].

4. Experimental results

Detailed measurements were carried out at 11 downstream stations starting as close as possible to the trailing edge: $\xi = x/\delta_m$ from 0^+ to 645 where x is the distance downstream and

$$\delta_m = \int_0^\infty U/U_0(1 - U/U_0)\, dy \quad \text{with} \quad \delta_m = 0.0026 \text{ m}, \tag{4.1}$$

with $\delta_m = 0.0026$ m at the trailing edge for the unheated flow case. Temperature differences of 0, 5, 16, 30 and 40°C were examined for both the upper flow heated (stable) and lower flow heated (unstable). From here on the terms stable and unstable will refer to the heating of the upper and lower flows respectively.

4.1. Mean flow quantities

The mean velocity and mean temperature profiles of the wake demonstrates self-preservation starting at $\xi = 176$. The data collapsed onto a single curve for all positions downstream as well as for neutral, stable and unstable temperature configurations with differences of 5, 16, 30 and 40°C. Mean velocity and temperature profiles at a fixed downstream station for varying temperature differences can be seen in Fig. 3a and 3b while for a fixed temperature difference at $\Delta T = 40$°C and varying downstream stations self-preserving mean velocity and temperature profiles are shown in Fig. 4a and 4b. The measured profiles were scaled by the self-preserving scales U_s and T_s, where $U_s = U_0 - U_{\min}$ and $T_s = T_h - T_0$, and where the subscript s refers to the maximum difference value, h the freestream maximum value and o the reference freestream. These are plotted against the non-dimensional coordinate $\eta = (y - y_0)/\delta_{0.5}$, where y_0 is the ordinate at which the velocity defect is maximum and $\delta_{0.5}$ is the wake half-width.

The self-preserved mean velocity profiles along the centerline provide a linear variation in mean velocity defect as a function of downstream as predicted THOMAS [74]. The present data when compared with the data of ALI and KOVASZNAY [2] as shown in Fig. 5, indicates good agreement with the linear fit for low temperature differences, say of the order of 16°C or below. Some variation from linearity begins to appear for larger temperature differences. Both the wake half-width and the centerline velocity defect followed the $x^{1/2}$ dependence.

The mean temperature profiles were monotonic in the cross-stream direction and the freestream values were held constant. These profiles demonstrate self-preservation while the scale T_s is a constant indicating that scaling is solely performed by η. The mean temperature slope along the centerline reaches its self-preserved state quickly and does not appear to show any markedly different features for low or high temperature differences.

The effect of buoyancy caused by mean temperature stratification is generally best

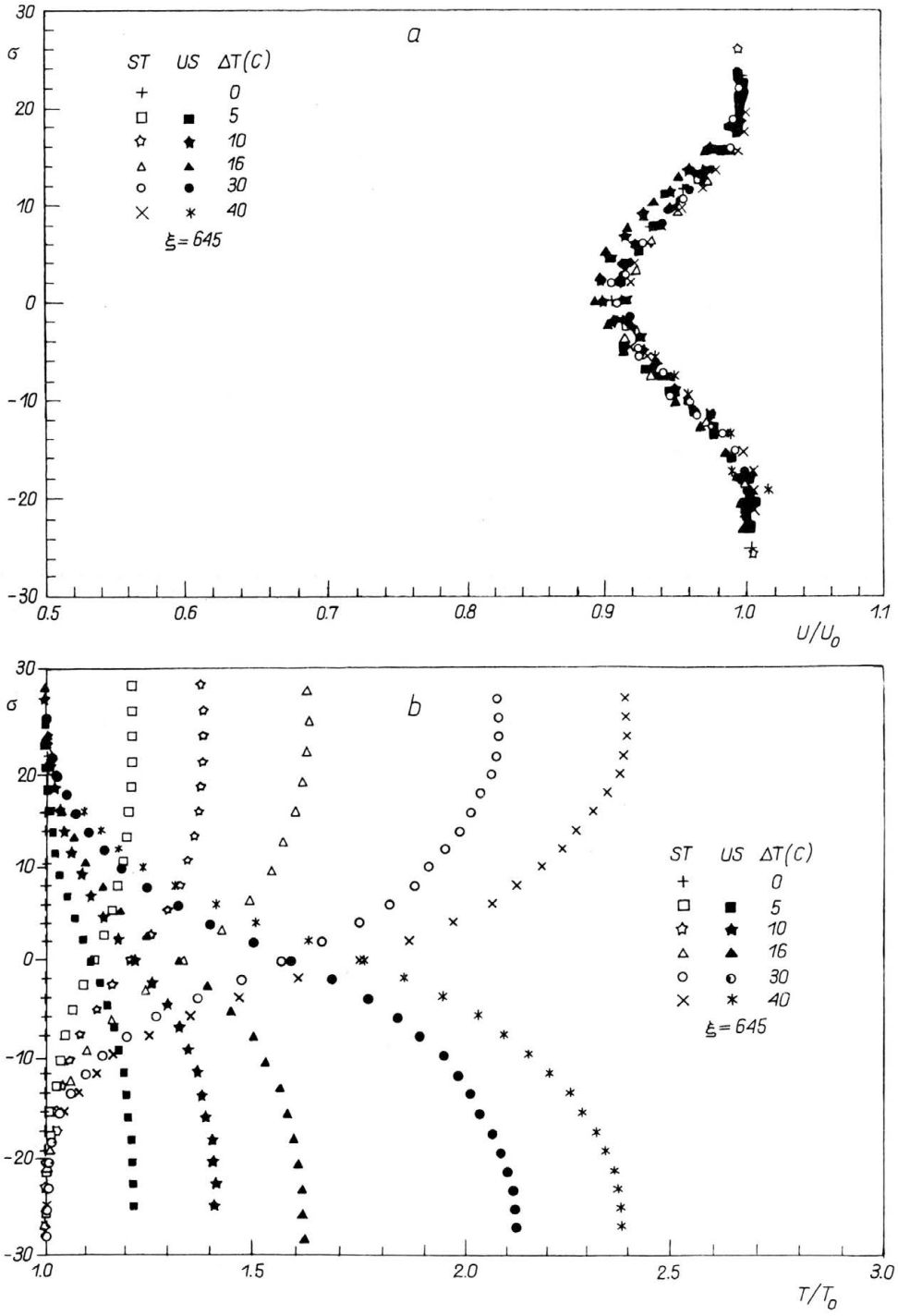

FIG. 3. a) Mean velocity and b) temperature profiles at a fixed downstream station $\xi = 645$.

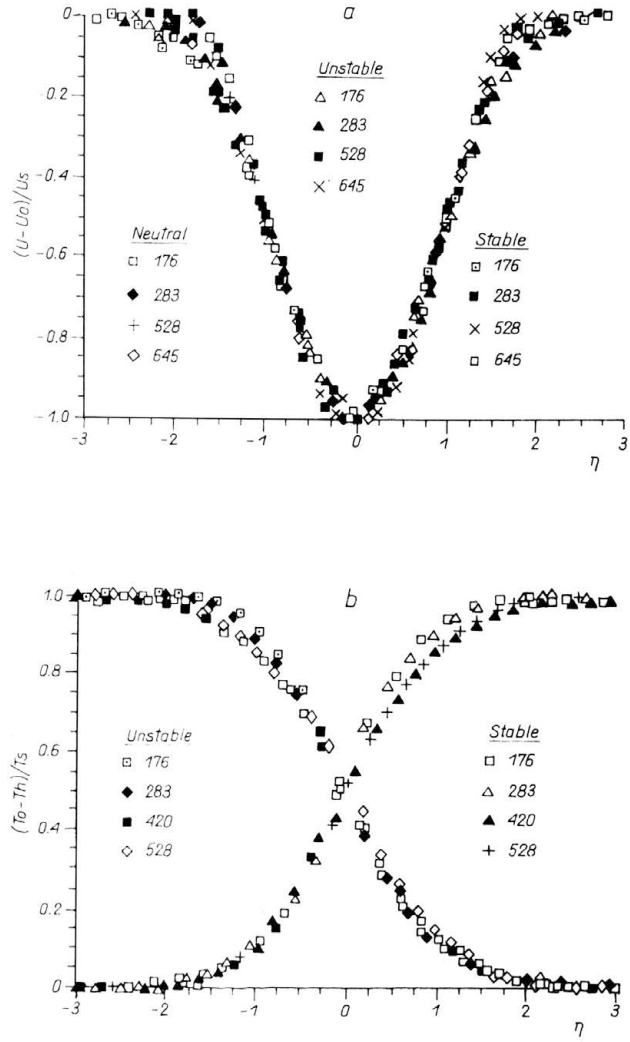

FIG. 4. Self-preserving, a) mean velocity and b) temperature profiles at downstream stations $\xi = 176, 283, 420, 528, 645$ for stable and unstable heating at $\Delta T = 40°C$.

indicated by the Richardson number

$$\text{Ri} = \frac{g}{T}\frac{\partial T/\partial y}{(\partial u/\partial y)^2}. \tag{4.2}$$

This local definition for our case clearly has some difficulties because the velocity gradient vanishes at the centerline and in the freestream. ALI and KOVASZNAY [2] and MOREL *et al.* [52, 53] suggested the use of average gradient Richardson number

$$\langle \text{Ri} \rangle = \frac{g}{T}\frac{T_s}{U_s}\frac{1}{(\partial T/\partial y)_{\max}}, \tag{4.3}$$

and found $\langle \text{Ri} \rangle$ to be in the range 0.1 and 4×10^{-4}, respectively, whereas in the present

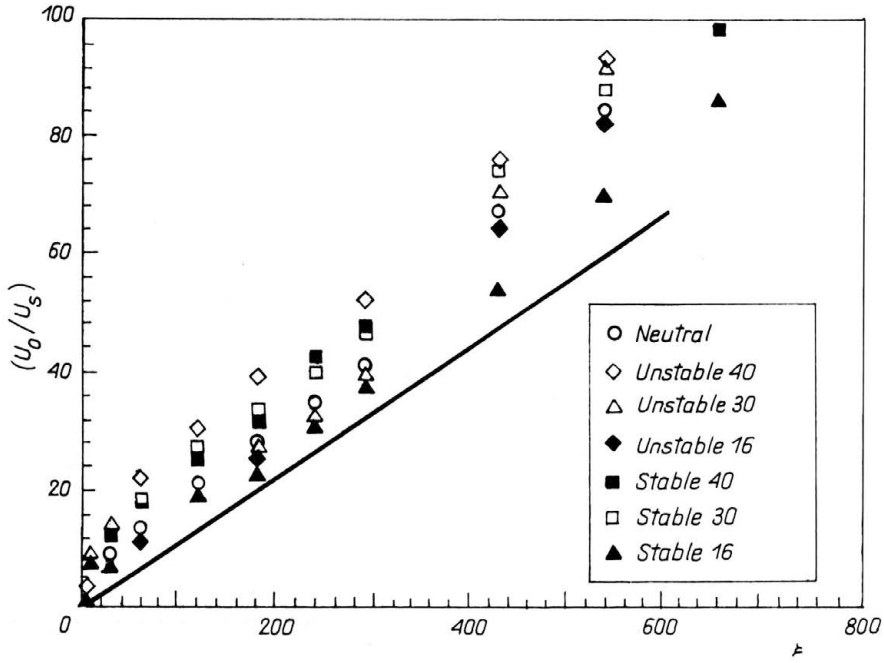

FIG. 5. Mean velocity defect along the centerline: solid line is reported by ALI and KOVASZNAY [2].

work $\langle \mathrm{Ri} \rangle$ was found to be slightly larger than 1. A better measure of the buoyancy effects can be obtained by examining the Brunt–Väisälä frequency, Nb. Typically, for a station $\xi = 645$, i.e. $x = 645\delta_m$ from the trailing edge the Brunt–Väisälä frequency is shown in Fig. 6. The extent of the velocity profile to within 99% of the freestream value is $-16 < \sigma < 16$, where $\sigma = y/\delta_m$. In this region for a $\Delta T = 40°\mathrm{C}$ the Brunt–Väisälä frequency range with stable stratification is $2.5 \leq Nb \leq 4.8$ and for unstable heating is $3.0 \leq Nb \leq 4.5$. Outside this region the profiles show a marked decay as the velocity and temperature fields approach their freestream values. The initial distribution is maintained in the central core of the flow. As can be seen the frequency distribution is skewed for both the stable and unstable cases for large temperature differences whereas for the lower heat input cases the distribution is symmetric.

4.2. Mean squared quantities

The rms streamwise velocity fluctuation for stable and unstable heating at a fixed downstream position $\xi = 645$ for varying temperature differences up to 40°C is shown in Fig. 7a. For lower heating rates the rms streamwise velocity fluctuation shows the classical double hump distribution with peak values of approximately 0.3 which are in good agreement with the data of ALI and KOVASZNAY [2]. For large temperature differences a change in the distribution occurs and the peak value increases up to three times the value for small temperature gradients. Similar results are obtained for stable and unstable temperature gradients at other downstream positions.

The vertical velocity fluctuation on the other hand shows substantial change in its

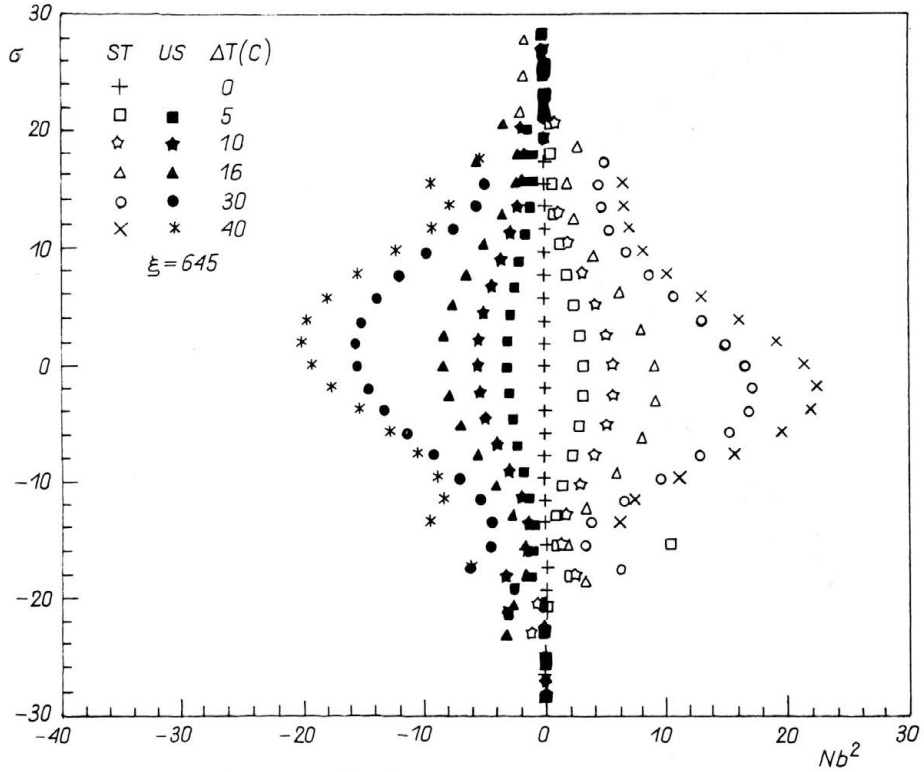

FIG. 6. Brunt—Väisälä frequency for all heating cases at $\xi = 645$. The sign can be appropriately accommodated by the sign of the temperature gradient.

distribution as seen in Fig. 7b. The rms vertical velocity fluctuation distributions are non-symmetric and skewed in the stable and unstable heating cases toward the maximum temperature gradient. Further, at high temperature gradients the distribution is concentrated at the thermal axis located away from the centerline whereas at low temperature gradients it is more broadly distributed about the flow centerline, i.e. the kinematic flow development axis.

While significant changes in the fluctuation velocity field are observed for stable and unstable temperature gradients, the rms temperature fluctuation develops rapidly from the trailing edge as seen in Fig. 8a. At fixed downstream positions only small changes in its distribution are observed. As the temperature difference is increased, the magnitude of the temperature fluctuation increases proportionally as seen in Fig. 8b. For small temperature differences, $\Delta T < 16°C$ the rms temperature fluctuation distribution is Gaussian and symmetric about the kinematic axis. For large temperature differences there is a shift in the temperature fluctuation distribution. The distribution is no longer symmetric but skewed to the heated side of the flow and the magnitude of its peak value has more than doubled. The skewness is similar to but not as distinct as that shown in Fig. 7b for the rms vertical velocity fluctuation. However, in both cases the shift is in the same direction. This shift in the thermal axis is consistent with the findings of MOREL *et al.* [53]. This observation reaffirms the independent character of the thermal field.

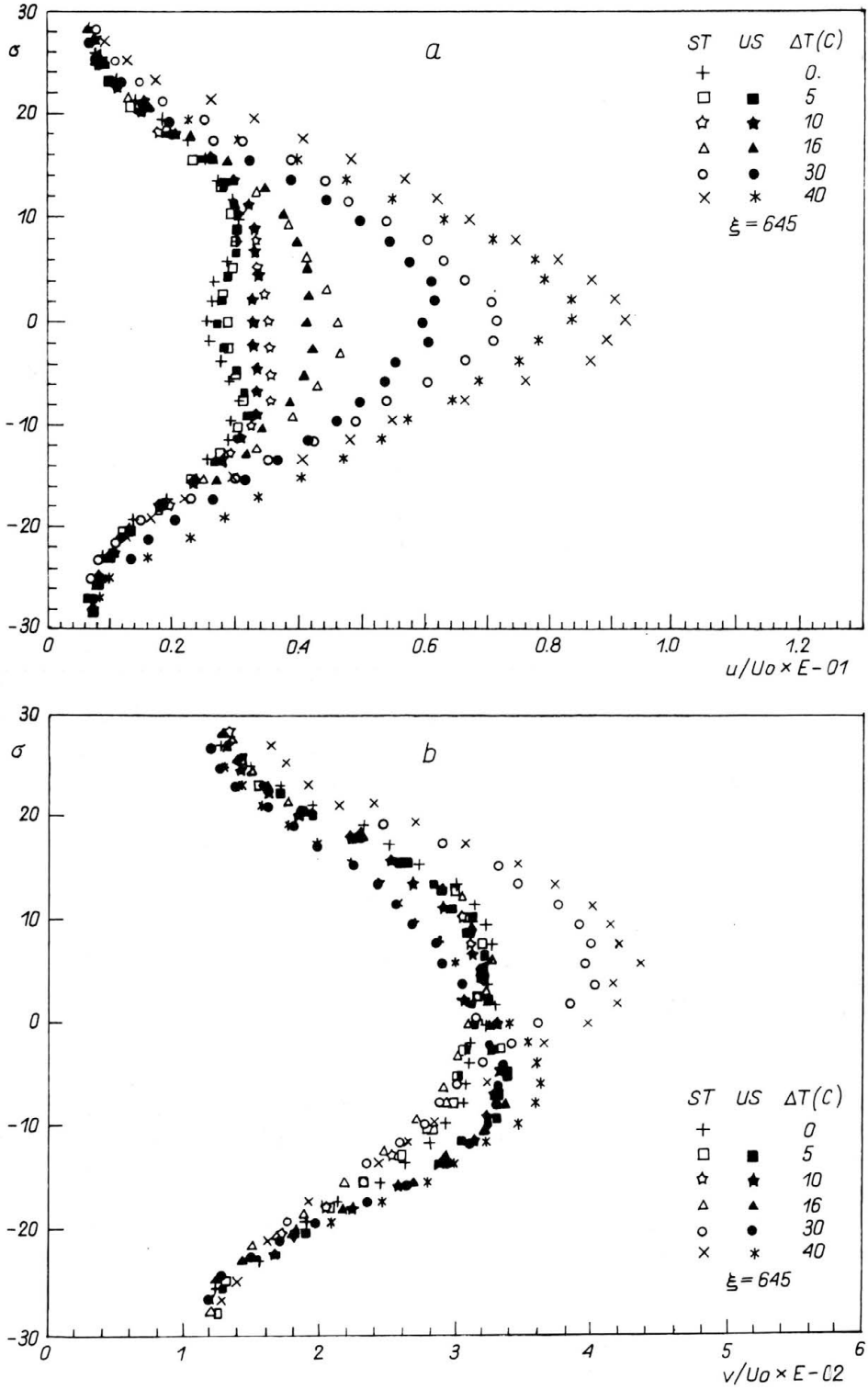

FIG. 7. RMS of a) streamwise velocity fluctuations and b) vertical velocity fluctuations for all heating cases, $\xi = 645$.

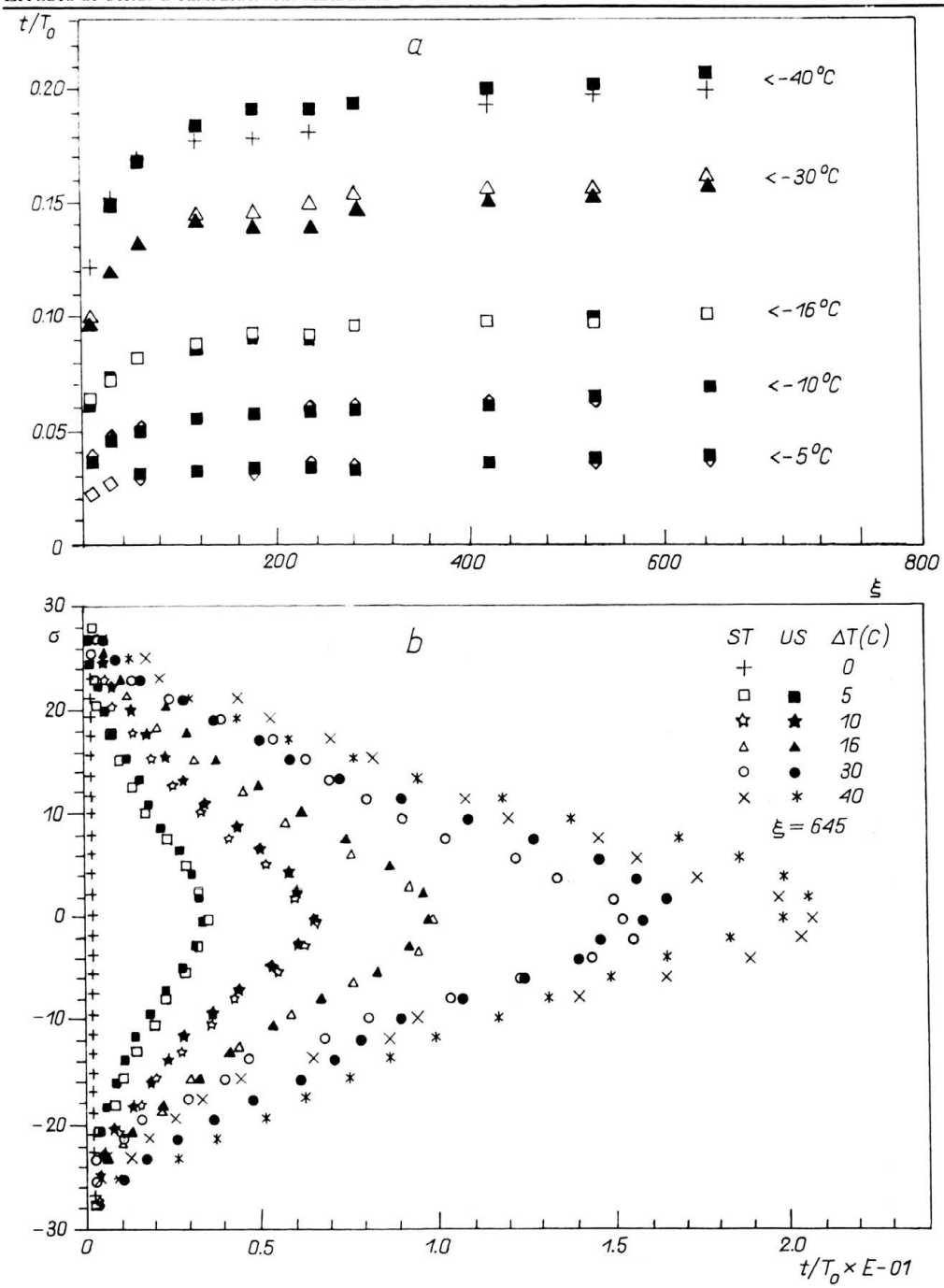

FIG. 8. a) Development of rms centerline temperature fluctuations with distance from the trailing edge, b) rms of the temperature fluctuations for all heating cases, $\xi = 645$.

4.3. Second-order cross-correlations

In the Reynolds decomposition the importance of second-order correlations cannot be understated because they relate to the streamwise and lateral transport of momentum and

heat. Of particular importance are the Reynolds stress $\overline{u'v'}$, and $\overline{u't'}$ and $\overline{v't'}$ contributions to the heat flux.

Since the wake is symmetric, all $\overline{u'v'}$ correlations are expected to be antisymmetric, e.g. see Fig. 9. Through the production term $\overline{v'^2}\partial\overline{U}/\partial y$ the Reynolds stress is fed directly by the velocity field. The $\overline{v'^2}$ distribution is non-symmetric and as a result contributes to a skewness in the Reynolds stress distribution. The maximum in the Reynolds stress occurs at the maximum in the $\overline{v'^2}$ distribution at which point the largest velocity defect gradient also occurs.

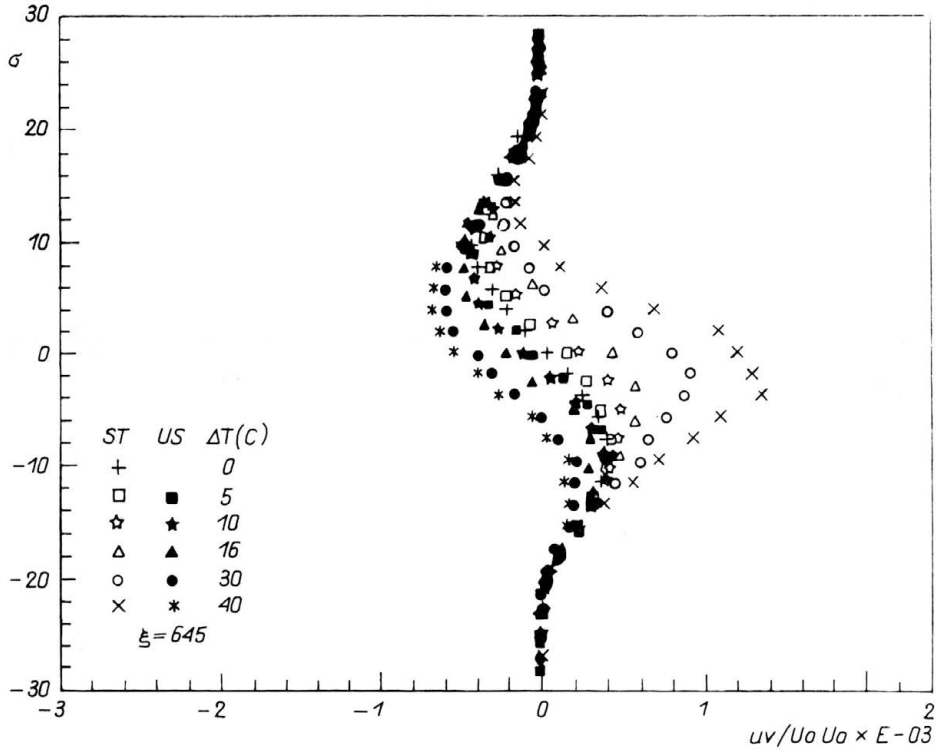

FIG. 9. Reynolds stress profiles for all heating cases, $\xi = 645$.

For small temperature differences the Reynolds stress at $\xi = 645$ has for all practical purposes attained self-preservation while at large temperature differences the Reynolds stress has not as yet reached this state. This same feature occurs in the $\overline{v'^2}$ distribution which contributes significantly to the Reynolds stress distribution. This feature that all correlations do not attain self-preservation at the same time is observed in general in free-turbulent shear flows, WYGNANSKI and FIEDLER [85].

The streamwise correlation $\overline{u't'}$ of the heat flux represents a minor portion of the total heat flux. The rms u' fluctuation shown previously is greater in the stable case than in the unstable one. As a result it is fed by the positive mean gradient and contributes to a larger streamwise heat flux with a tendency for more heat transfer in the steeper gradient portion of the flow.

The $\overline{v't'}$ correlation represents the cross-stream transport of heat per unit area in vertical planes. Its product with the lateral gradient of temperature is responsible for the main production rate of temperature fluctuation $\overline{t'^2}$. This production is governed by the interaction of the thermal field $\partial\overline{T}/\partial x_i$ and the temperature correlation $\overline{u_i't'}$. These terms as a rule are positive, however, they are strongly governed by the signs of $\overline{v'^2}$ and $\partial\overline{T}/x_i$. For example, in the unstable case the lateral diffusion of t' is a normal distribution curve slightly skewed toward the strongly heated lower flow at large temperature differences as shown in Fig. 8b. The vertical correlation $\overline{v't'}$ has a skewed distribution toward the lower portion of the flow where the temperature gradient manifests itself as seen in Fig. 10. The skewness is caused by the slightly skewed temperature fluctuation distribution and the strongly skewed vertical velocity fluctuation distribution which again causes the thermal axis to differ from the kinematic development axis of the wake.

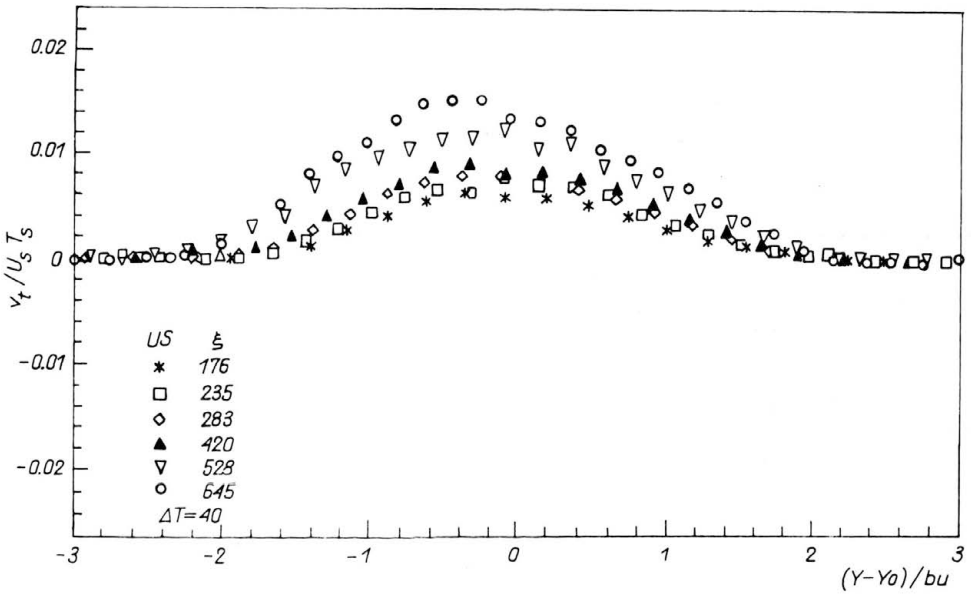

FIG. 10. Vertical heat flux distribution for unstable heating at $\Delta T = 40°C$.

It is interesting to note that, while both $\overline{u't'}$ and $\overline{v't'}$ carry both kinematic and thermal information, they are of a different nature. The $\overline{u't'}$ correlation depends primarily on the large scale structure which is strongly linked to initial flow conditions whereas the smallest structures are necessarily linked the Kolmogorow length scale, i.e. linked to the kinematic field. The $\overline{v't'}$ correlation principally depends on the small structure and the variance of $\overline{v'^2}$ which is part of the production term $v'^2\partial\overline{T}/\partial y$. It is produced by the interaction of $\overline{v'^2}$ with the mean temperature gradient in the same way the Reynolds stress is fed directly through $\overline{v'^2}\partial\overline{U}/\partial y$.

4.4. Kinetic energy

To examine the effects of the mean temperature field on the turbulent energy we examine the total fluctuation energy density, see e.g. MONIN and YAGLOM [50]. The mean

fluctuation energy density is obtained by taking the time average of the instantaneous term $1/2\tilde{\rho}\tilde{u}'\tilde{u}'$ and the Reynolds decomposition for $\tilde{u}_i = V_i + u_i'$ and $\tilde{\rho} = \rho + \rho'$. This results in

$$E = E_t + E_{st}\,, \tag{4.4}$$

where E_t is the energy density of the fluctuating motion

$$E_t = 1/2(\rho\overline{u_i'u_i'} + \overline{\rho' u_i'u_i'})\,, \tag{4.5}$$

where E_{st} is the transport of the $\overline{\rho' u_i'}$ by the mean motion U_i

$$E_{st} = \overline{\rho' u_i'}U_i\,. \tag{4.6}$$

Since we cannot directly measure the fluctuating density, the Boussinesq approximation $\delta'\alpha t'$, where t' is the temperature fluctuation, is employed. This leads to

$$E_t = 1/2[\rho(\overline{u'^2} + \overline{v'^2}) - (\rho g/T)(\overline{u'^2t'} + \overline{v'^2t'})]\,, \tag{4.7}$$

and

$$E_{st} = -(\rho g/T)(U\overline{u't'} + V\overline{v't'})\,. \tag{4.8}$$

For large temperature fluctuations the use of the Boussinesq approximation is questionable, however, direct measurement of the three terms in Eqs. (4.5) and (4.6) provides evidence that the triple correlation term is two orders of magnitude smaller when compared to the other terms, thus the energy density becomes $E_t = 1/2\rho\overline{u_i'u_i'}$.

The initial profiles for the kinetic energy density are very similar for both stable and unstable stratification and can be seen in Fig. 11 for a stably heated flow. The data is non-dimensionalized as $E_t^* = E_t/\rho_a U_0^2$ where ρ_a is the average of the upper and lower stream densities. For a fixed position downstream, well into the self-preservation flow regime, as the temperature increases, the energy density profiles change from classical constant property bimodal distribution to a single peak distribution profile which is skewed from the centerline as shown in Fig. 12.

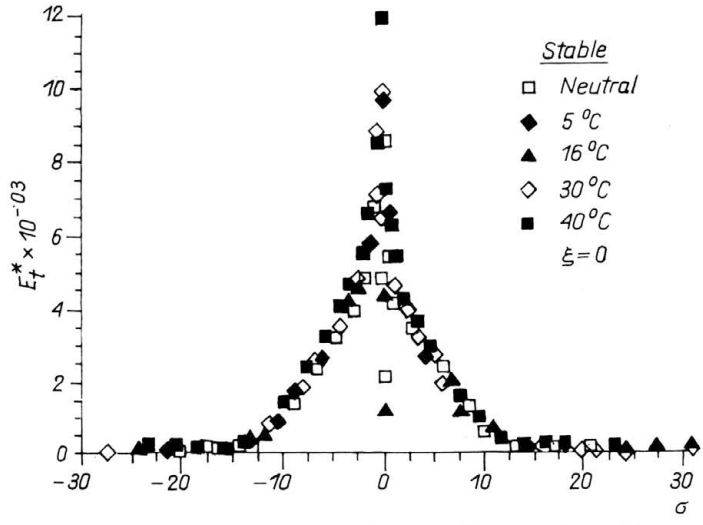

FIG. 11. Kinetic energy density, upper flow heated, $\xi = 0^+$.

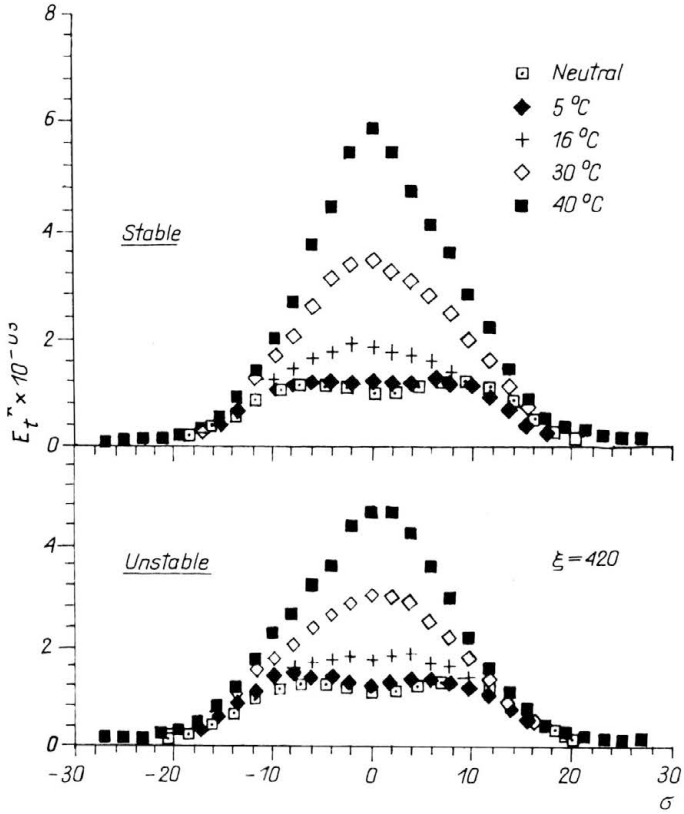

FIG. 12. Temperature effects on the local E_t^* profiles at downstream station $\xi = 420$.

Further information on the effects of temperature on the development of E_t can be obtained from the integral value of the E_t defined as

$$E_t = \frac{1}{2} \int_{-\infty}^{\infty} \frac{U}{U_0} \rho \overline{u_i' u_i'} \, dy \,. \tag{4.9}$$

In Fig. 13 for $\Delta T = 5°C$ buoyant production appears to be contributing as expected in that the unstably heated data have larger integrated energy densities than the stably heated results. As the temperature is increased to 16°C, the integrated energy densities are of the same order of magnitude but their relative positions have changed indicating the temperature field is no longer passive but is responsible for dynamically active buoyancy forces which feed energy into the fluctuating velocity field. The magnitude of the energy exchange increases rapidly for $\Delta T's > 16°C$ as shown in Fig. 14. The local production of turbulent energy takes place in the "active" core region where there exists significant fine-scale mixing and the dynamically active buoyancy forces tend to predominate. A similar integration preformed on the $\overline{\rho' u' U}$ term results in the a negative contribution to the overall energy density as the temperature increases above 16°C indicating less production by the gradient of the larger scale motions.

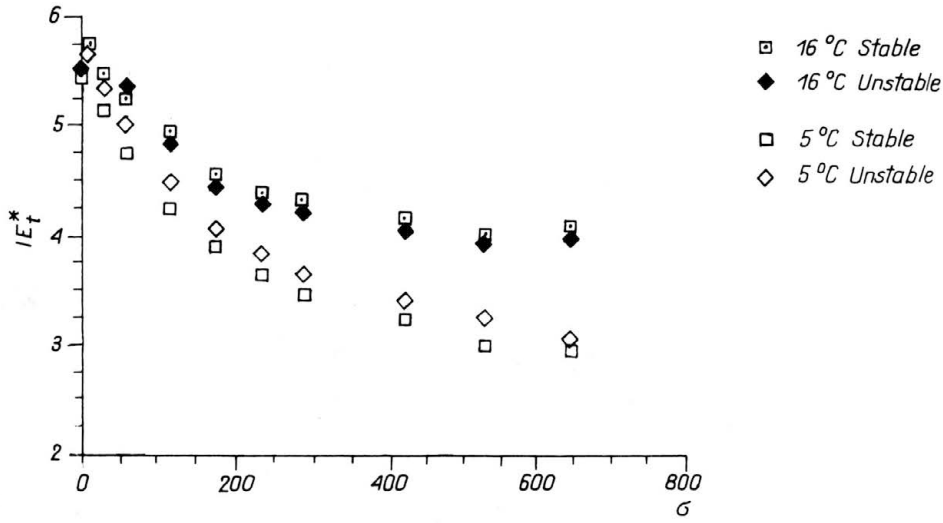

FIG. 13. Integrated E_t^* profiles for the 5°C and 16°C cases.

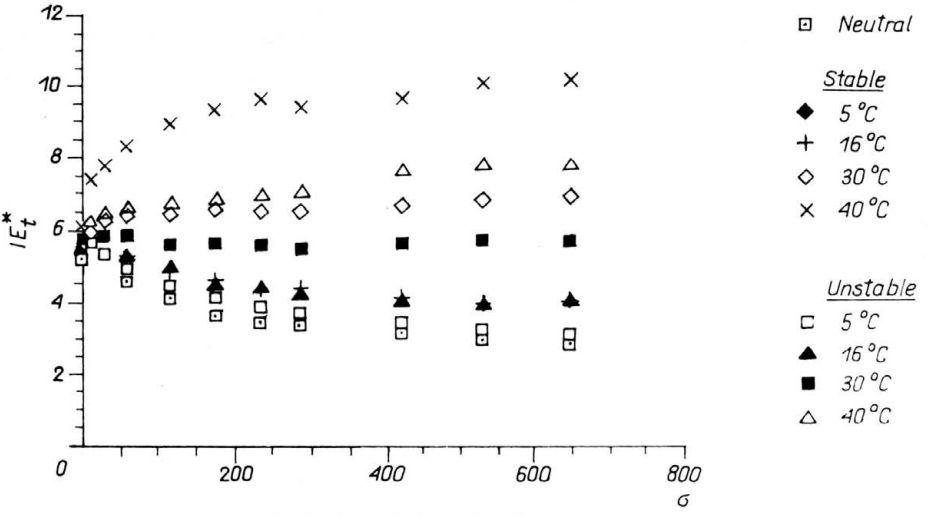

FIG. 14. Integrated E_t^* profiles for all temperature cases.

5. Summary and conclusion

Results of experiments on a developing wake behind a splitter plate in the presence of strong temperature stratification have been presented. In general the mean velocity profile was not significantly affected by a strong temperature stratification field imposed as the wake growth and velocity defect followed the $x^{1/2}$ law.

The mean temperature field developed rapidly and the mean velocity and tempera-

ture profiles indicated self-preservation at a distance of approximately 175 momentum thicknesses downstream of the trailing edge. This was true for the entire range of temperature stratification, Brunt–Väisälä frequencies, 2 – 6 rad/sec. While the mean velocity and temperature were self-preserved, the turbulent stresses, higher-order correlations and energies, especially for large temperature differences, did not in general demonstrate the same self-preservation (within the wake downstream distances investigated).

For small temperature differences, as expected, stable stratification dampened the turbulence while unstable stratification tended to augment it. For large temperature differences this was not the case as the effects of dynamically active buoyancy forces played a significant role in the process. Energy density magnitudes increased 5 to 6 times the levels of that of isothermal flow and a strongly maintained temperature gradient fed the development of the temperature fluctuations as well as the overall turbulence field. It appears from the present work that for temperature differences of $< 16°C$ the imposed temperature stratification is passive while for larger temperature differences the dynamically active buoyancy forces contribute significantly to the kinetic energy density.

Finally, the thermal structure displays some independence with respect to the kinematic wake. This is particularly true for the velocity-temperature correlations at large temperature differences, where the integral temperature and the integral velocity scales vary in different ways. Hence, the thermal wake has its own signature.

6. Acknowledgements

The author acknowledge, with appreciation, the support of the present work by the U.S. National Science Foundation under Grant CBT 82-13456-02. Also the senior author acknowledges the support of the National Science Foundation under Grant CTS 89-18611 for travel funds to present this paper at the XIXth Biennial Fluid Dynamics Symposium held in Kozubnik, Poland in September 4–8, 1989, and of the Polish Academy of Sciences during his stay in Poland.

References

1. C.C. ALEXOPOULOS and J.F. KEFFER, Rep.6811, University of Toronto, 1968.
2. S.F. ALI and L.S.G. KOVASZNAY, AFOSR–TR–75–1657, 1975.
3. J. ANDREOPOULOS and P. BRADSHAW, J.Fluid Mech., **100**, 639, 1980.
4. R.A. ANTONIA, H.Q. DANH and A. PRABHU, J.Fluid Mech., **80**, 153, 1970.
5. R.A. ANTONIA and C.W. VAN ATTA, J.Fluid Mech., **67**, 273, 1975.
6. R.A. ANTONIA, A.J. CHAMBERS, D. BRITZ and L.W.B. BROWNE, J.Fluid Mech., **172**, 211, 1986.
7. R.A. ANTONIA, L.W.B. BROWNE and D.K. BISSET, J.Fluid Mech.,**184**, 423, 1987.
8. R.A. ANTONIA, L.W.B. BROWNE, D.K. BISSET and L. FULACHIER, J.Fluid Mech, **184**, 423, 1987.
9. R.A. ANTONIA, L.W.B. BROWNE and D.A. SHAH, J.Fluid Mech., **189**, 349, 1988.
10. S.P.S. ARYA, J.Fluid Mech., **68**, 321, 1975.
11. N.I. BOLONOV and V.G. LOBACHEV, Ht. Trans. Soviet Res., **13**, 75, 1981.
12. M.L. BARSOUM, J.G. KAWALL and J.F. KEFFER, Phys. Fluids, **21**, 157, 1978.
13. E. BERGER and R. WILLE, Ann. Rev. Fluid Mech., **4**, 313, 1972.
14. L.P. BERNEL, Ph.D.Thesis, California Institute of Technology, 1981.
15. L.J.S. BRADBURY, J.Fluid Mech. **23**, 31, 1965.
16. F.K. BROWAND, J.Fluid Mech., **26**, 281, 1966.
17. F.K. BROWAND and P.D. WEIDMAN, J.Fluid Mech., **76**, 127, 1976.
18. F.K. BROWAND and C.M. HO, J.Mec.Theor.Appl., **99**, 1987.
19. L.W.B. BROWNE, R.A. ANTONIA and D.A. SHAH, J.Fluid Mech., **179**, 307, 1987.

20. L.W.B. BROWNE, R.A. ANTONIA and D.K. BISSET, Phys.Fluids, **29**, 3612, 1986.
21. R. CANTWELL and D. COLES, J.Fluid Mech., **136**, 321, 1983.
22. R. CHEVREY and L.S.G. KOVASZNAY, AIAA, **7**, 1641, 1969.
23. J.M. CIMBALA, Ph.D.Thesis, California Institute of Technology, 1984.
24. J.M. CIMBALA, Proc. Fifth Symp. on Turbulent Shear Flows, Cornell Univ., 4.1. 1985.
25. J.M. CIMBALLA, H.M. NAGIB and A. ROSHKO, J.Fluid Mech., **190**, 265, 1988.
26. J. COHEN, E. GUTMARK and I. WYGNANSKI, AIAA J., **21**,1983.
27. S. CORRSIN, NACA, WR-94, 1947.
28. S. CORRSIN and M. UBEROI, NACA Rep. 998, 1950.
29. A.E. DAVIES, J.F. KEFFER and W.D. BAINES, Phys. Fluids, **18**, 770, 1975.
30. P.E. DIMOTAKIS and G.L. BROWN, J.Fluid Mech., **78**, 535, 1976.
31. G. FABRIS, Ph.D.Thesis, Illinois Institute of Technology, 1974.
32. G. FABRIS, J.Fluid Mech., **673**, 1979.
33. J.A. FERRE and F. GIRALT, J.Fluid Mech., **65**, 1989.
34. P. FREYMOUTH and M.S. UBEROI, Phys. Fluids, **12**, 1359, 1969.
35. P. FREYMOUTH and M.S. UBEROI, Phys. Fluids, **14**, 2574, 1971.
36. V. GOLDSCHMIDT and M.F. YOUNG, Rep. HL 73-31 Purdue University, 1973.
37. H.L. GRANT, J.Fluid Mech., **4**, 149, 1958.
38. E. GUTMARK and I. WYGNANSKI, J.Fluid Mech., **73**, 465, 1976.
39. P.E. JENKINS, Ph.D.Thesis, Purdue University, 1975.
40. J.F. KEFFER, J.Fluid Mech., **22**, 135, 1965.
41. J.F. KEFFER, J.Fluid Mech., **28**, 183, 1967.
42. N.E. KOTSOVINAS, Ph.D.Thesis, California Institute of Technology, 1975.
43. L.S.G. KOVASZNAY, Proc.Roy.Soc., **A198**, 174, 1948.
44. J.C. LARUE and P.A. LIBBY, Phys.Fliuds, **17**, 873, 1974.
45. J.V.H. LIENHARD and C.W. VAN ATTA, Paper subm. to J.Fluid Mech., Prepublication copy; U.Cal. at San Diego, LaJolla.CA, 1988.
46. J.V.H. LIENHARD and C.W. VAN ATTA, Exp. in Fluids, **7**, 542, 1989.
47. H.W. LIEPMANN and J. LAUFER, NACA Tech. Note, 1257, 1947.
48. E. MAYER and D. DIVOKY, AIAA, 4, 1995, 1966.
49. H. MAECKEWA, Rep.Dept.ME Engr., Kagoshima Univ., Japan, 1988.
50. A.S. MONIN and A.M. YAGLOM, *Statistical fluid mechanics Mechanics of turbulence*, MIT Press, Cambridge 1973.
51. R. MOREL, M. AWAD, J.P. SCHON and J. MATHIEU, Structure and Mech. of Turbulence., I,36, Berlin 1978.
52. R. MOREL, M. AWAD, J. MATHIEU and J.P. SCHON, Phys. Fluids, **22**, 623, 1979.
53. R. MOREL, C. REY and J.M. WALLACE, J.Fluid Mech., **26**, 416, 1983.
54. M. MORKOVIN, Proc. ASME Symp., 102, 1964.
55. J.C. MUMFORD, J.Fluid Mech., **137**, 447, 1983.
56. R. NARASHIMA and A. PRABHU, J.Fluid Mech., **54**, 1, 1972.
57. C.I.H. NICHOLL, J.Fluid Mech., **40**, 361, 1970.
58. P.H. OOSTHUIZEN, ASME Paper 77-WA/HT-31. 1978.
59. D.D. PAPAILIOU and P.S. LYKOUDIS, J.Fluid Mech., **62**, 11, 1974.
60. B.R. RAMMAPRIAN and V.C. PATEL, AIAA, 7, 1641, 1981.
61. C. REY, J.P. SCHON and J. MATHIEU, C.R.Acad.Sci., **281**, 215, Paris 1975.
62. C. REY, J.P. SCHLON and J. MATHIEU, Phys.Fluids, **22**, 1020, 1979.
63. A. ROSHKO, NACA TN 2913, 1953.
64. A. ROSHKO, AIAA, 76–78, 1976.
65. A. ROSHKO, *In the role of coherent structures in modelling, turbulence and mixing*, Lecture Notes in Phys., Springer, 136, 208, Berlin-Heidelberg-New York 1981.
66. J.P. SCHON, C. REY, P. MERY and J. MATHIEU, Heat Trans. and Turb. Buoyant Centre, 1, 211. 1977.
67. B.W. SPENCER, Ph.D.Thesis, University of Illinois, 1970.
68. K.R. SREENIVASAN, AIAA J., **19**, 1365, 1981.
69. K.R. SREENIVASAS and R. NARASHIMA, J.Fluid Mech., 104, 167, 1982.
70. C.R. SYMES and L.E. FINK, Structures and Mechanisms of Turbulence 1, 86, Berlin 1977.
71. S. TANEDA, J.Phys.Soc.Japan, **14**, 843, 1959.
72. S. TAVOULARIS and S. CORRSIN, J.Fluid Mech., **311**, 1981.

73. S. TAVOULARIS and K.R. SREENIVASAN, Phys.Fluids, **24**, 778, 1981.
74. R.M. THOMAS, J.Fluid Mech., **57**, 549, 1973.
75. A.A. TOWNSEND, Aust.J.Sci.Res., 1, 161, 1948.
76. A.A. TOWNSEND, Proc.Roy.Soc.London, A190, 551, 1947.
77. A.A. TOWNSEND, Proc.Roy.Soc.London, A197, 124, 1949a.
78. A.A. TOWNSEND, Aust.J.Sci.Res., 2, 451, 1949b.
79. A.A. TOWNSEND, *The structure of turbulent shear flow*, 2nd Ed., Cambridge University Press, London 1956.
80. A.A. TOWNSEND, J.Fluid Mech., **95**, 515, 1979.
81. T.F. TUREAUD, Ph.D.Thesis, Univ. of Notre Dame, 1988.
82. T.F. TUREAUD, A.A. SZEWCZYK, V.W.Nee and K.T.Yang, Proc. 1st World Conf. on Exp. Heat Transfer, Fluid Mech and Thermo, Yugoslavia 1988.
83. M.S. UBEROI and P. FREUMUTH, Phys.Fluids, **12**, 1359, 1979.
84. Z. WARHAFT and J.L. LUMLEY, J.Fluid Mech., **88**, 659, 1978.
85. I. WYGNANSKI and H.E. FIEDLER, J.Fluid Mech., **38**, 577, 1969.
86. I. WYGNANSKI, H.E. FIEDLER, J. Fluid Mech., **41**, 237, 1970.
87. I. WYGNANSKI, F.H. CHAMPAGNE and B. MARASLI, J.Fluid Mech., **168**, 31, 1986.
88. H. YAMADA, Y. KAWATA, H. OSAKA and V. KAGEYAMA Tech.Reports of the Yamaguchi Univ. Japan, **2**, 4, 1980.
89. K.B.M.Q. ZAMAN and A.K.M.K. HUSSAIN, J.Fluid Mech., **112**, 379, 1981.

DEPARTMENT OF AEROSPACE AND MECHANICAL ENGINEERING
UNIVERSITY OF NOTRE DAME, INDIANA, USA.

Received August 26, 1991.